



Mitigation of Flash Flood Hazards Through the Optimum Utilization of Surface Water Harvesting Techniques of Wadi Abu Safaa, Northwest of El Shalateen Area, Red Sea, Eastern Desert, Egypt

BY

Ismail, Y.L¹., Nahla A. Morad¹, Hozien, A² and Abd El Latif, R.M¹.

1. Hydrology Department, Desert Research Center, Cairo, Egypt

2. Environmental Department, Desert Research Center, Cairo, Egypt

ABSTRACT

Flood prevention and mitigation strategies can be facilitated by flood susceptibility mapping (FSM), since it signifies regions with the greatest risk according to physical attributes. Therefore, the current work aims to evaluate the susceptibility to flood hazards in the Abu Safaa watershed. For locating and evaluating possible hazardous zones, nine criteria, namely elevation, slope, flow accumulation, rainfall intensity, distance from drainage, drainage network density, TWI, LULC, and NDVI, were integrated into ArcGIS. A mathematical method for modeling flood hazards and providing decision assistance that considers the weighting and ranking for each flood criteria is called the analytical hierarchy process (AHP), which is used to obtain the Flood Hazard Index (FHI), flash flood hazard zones (FFHs), and then generate a flood susceptibility map. Five assessments of flood potential are detected, ranging from extremely low to very high: 11.21% (very low), 26.5% (low), 32.81% (moderate), 20.18% (high), and 9.3% (very high). For flood mitigation purposes, FSM and the selected morphometric parameter results were used to conduct a weighted spatial probability model to figure out probable regions for capturing rainwater, as well as the proposed strategy with suitable locations of water harvesting structures for direct usage as surface water storage, indirect usage as groundwater recharge, or a combination of both. The present study's findings show that the Abu Safaa basin accepted $61.4 \times 10^6 \text{ m}^3$ of rainfall in February 2018, which led to a water harvesting potential of about $10.3 \times 10^6 \text{ m}^3$ and total losses of about $51.1 \times 10^6 \text{ m}^3$.

Keywords: susceptibility; multicriteria decision analysis; hazard; flash flood mitigation; rainwater harvesting.

INTRODUCTION

The Egyptian resort town of Sharm el-Sheikh will host the climate change summit (COP27) in November 2022. Because the climate summit is being held in an African country, it is opportune to focus on African climate change research (Al-Zu'bi et al., 2022). In the past few years, the implications of floodwaters have increased globally when unusual storms originating from changing climates are modifying the pattern of rainfall (Rajkhowa and Sarma 2021). Equitably essential, but acquiring fewer considerations, is the fact that growing population, accelerated urbanization, and economic progress in areas vulnerable to floods are worsening flooding hazards. The increasing frequency of flood events is largely the result of continuous climatic changes, as well as alterations in land use caused by human activities. Furthermore, human activities frequently restrict basins' natural retention and modification abilities, which can contribute to hastened surface discharge or processes of erosion (Costache et al., 2014). In present-day society, managing water resources and the hydrological hazards associated with them is becoming more

important. Wadi Abu Safaa is considered a vibrant and prospective catchment in southeastern Egypt. It is in the northwest part of El Shalateen city, between latitudes 23°6' to 23°31' N and longitudes 34°28' to 34°58' E (Figure 1). Wadi Abu Safaa catchment has an area of 1204 km², a perimeter of about 258.37 km, and a basin length of about 48 km.

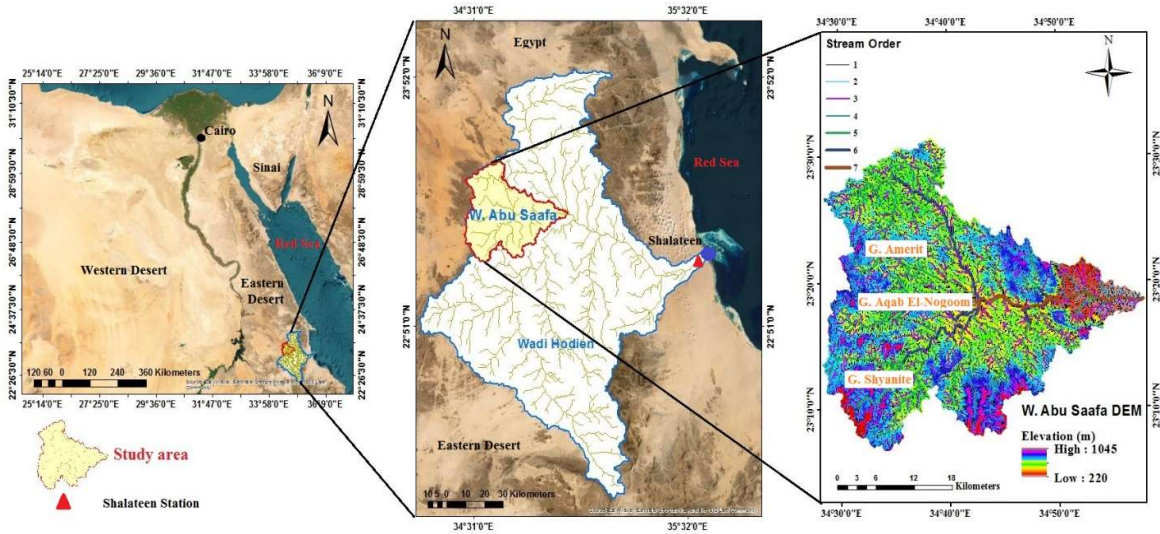


Fig. 1: Location map of the study area

Bedouin local residences in Abu Safaa, along with various development projects (i.e., mining, tourism, etc.), rely primarily on natural springs and wells dug by hand and haven't got adequate water supplies to meet their requirements. They suffer from flash flood damage, and their reliance on the accessible water resources is extreme and will rise owing to population expansion.

According to the available meteorological data (1999–2018) from Shalateen Station (Deseret Research Center) (Figure 1), Wadi Abu Safaa is classified as arid, with an average rainwater of 10 mm from October to December (Figure 2) and practically no precipitation throughout the remainder of the year. Thunderstorms and sporadic rainfall during the spring and fall seasons can occur sporadically. Many flash floods occurred in the previous few years, causing substantial infrastructural destruction, population relocation, and even death. The availability of surface water during a flash flood may be used as a possible supply of water rather than a disaster phenomenon. The purpose of the current research is to perform accurate mapping of flood susceptibility regions in the Abu Safaa basin using the Geographic Information System (GIS) integrated through the Analytical Hierarchy Process (AHP), a multi-criteria decision analysis (MCDA) approach for identifying zones of flash flood hazards (FFHs). As a result, susceptibility can be viewed as one of the measures of risk evaluation (Nsangou, 2022). Flood Susceptibility Mapping (FSM) and natural hazard assessment techniques, in general, depend upon a variety of influencing factors which reflect the physical features within the researched region. Land use/cover,

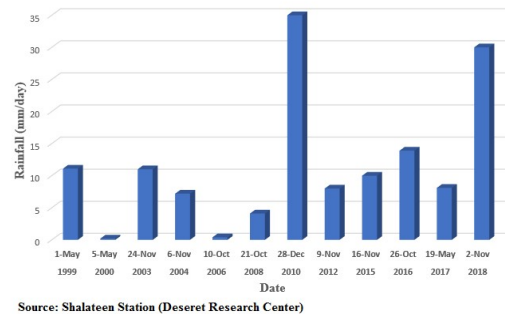


Fig. 2: Annual maximum daily rainfall (mm) events for the study area (2000 - 2018)

Mitigation of Flash Flood Hazards Through the Optimum Utilization of Surface Water Harvesting Techniques of Wadi Abu Safaa, Northwest of El Shalateen Area, Red Sea, Eastern Desert, Egypt

morphometric features (e.g., elevation, slope), precipitation, various categories of soil or hydrological soil groups, river network density, geology or lithology, and similar criteria are often utilized.

GIS facilitates spatial data processing and analysis, as well as the visual representation, explanation, and assessment of AHP outcomes. Because floods are multi-dimensional phenomena, multi-criteria decision analysis (MCDA) has become a method employed in determining the corresponding significance of the chosen aspects of conditioning (Souissi et al., 2019). In addition, for validation purposes, GIS-integrated recordings of flood occurrences involving historical flood locations where leastwise one flood event occurred between 1901 and 2022 were used. Flood susceptibility mapping and assessment, on the other hand, is a crucial aspect of flood mitigation and preventative techniques since it reveals highly hazardous areas based on physical parameters that indicate flooding potential. Water catchment structures reduce the velocity of water during flash flood events by increasing the time of concentration of the hydrographic basins and lowering the flood peak. Sites for water harvesting techniques and mitigation are suggested for possible implementation in Wadi Abu Safaa for flood mitigation. RWH structures reduce water velocity during flash flood episodes by enhancing the time of concentration in the investigated regions and lowering the flood peak. As soon as water is kept in the Abu Safaa catchment (through storage and percolation), it may decrease the quantity of runoff generated and increase storage capacity in the Quaternary aquifer and the exposed Nubian Sandstone aquifer, which are heavily used by the area's farmers.

GEOLOGICAL SETTING

Several researchers discovered the geologic attitude of the mega-basin Hodein region: Hassan and Masoud (2015) and Awad et al. (2021). The basement (metamorphic and intrusive) and sedimentary rocks, as well as Tertiary basalts, occupy the subbasin Abu Safaa (Figure 3). A large portion of the southern region is made up of Late Proterozoic Precambrian basement rocks. Conversely, non-conformably, small beds of Cretaceous sandstones cover the basement rocks. Two geologic formations belonging to the Nubia Group (or "Sandstone") of Cretaceous age, the Umm Barmil and Timsah, comprise the bedrock exposed in the hills around Bir Abu Safa. The Umm Barmil Formation is more porous and permeable than the underlying Timsah Formation. Rain falling infiltrates into the Umm Barmil and moves downward until it reaches the Timsah Formation.

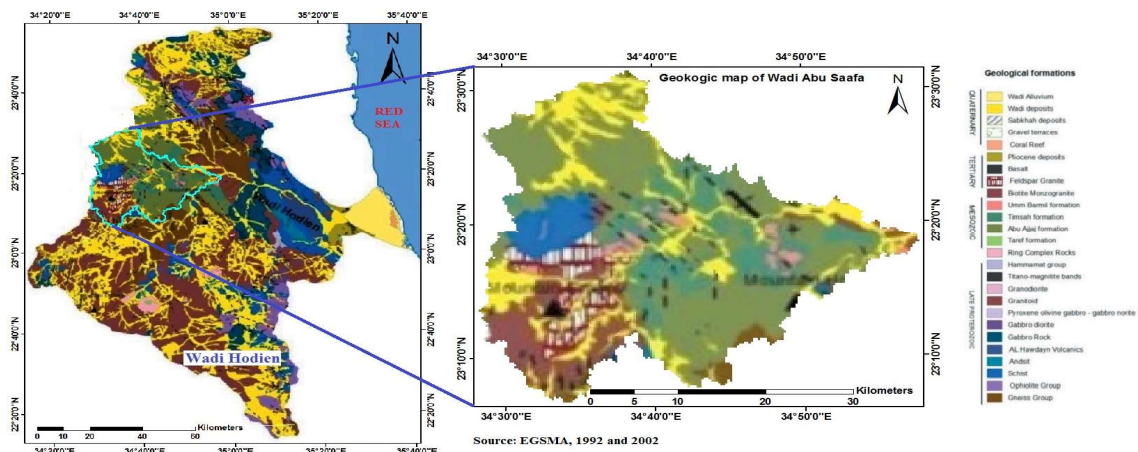


Fig. 3: Geologic map of the Wadi Abu Safaa Catchment area

HYDROGEOLOGICAL SETTING

Generally, four main geologic units, in general, represent the water bearing formations in the Eastern Desert: the Quaternary, the Nubian sandstone, the fractured limestone and sandstone, and the fractured crystalline Pre-Cambrian aquifer. (Zaghloul, 1996) and. Consequently, the study area's two main aquifers—the Quaternary and upper Cretaceous—were identified as potential aquifers, with the Precambrian-aged secondary aquifer being the third. The first probable aquifer is Quaternary in age and consists of wadi fill deposits, Pleistocene alluvial sands and gravels, and Holocene sand layers and dunes of sand along the courses of many of today's basins. The next possible aquifer is of upper Cretaceous age and has been identified as the Nubian sandstone aquifer owing to scattered outcrops of fluvial sandstone from the Umm Barmil and Timsah Formations; the third is the secondary aquifer that originated from reworked fragmented and fissured granitoid rocks of Precambrian age (Fig. 4). Unconformable and/or structurally controlled connections between Pre-Cambrian basement rocks and Cretaceous sandstone, as well as between Quaternary deposits and Cretaceous sandstone outcrops, support the concept that these three aquifers are hydraulically connected.

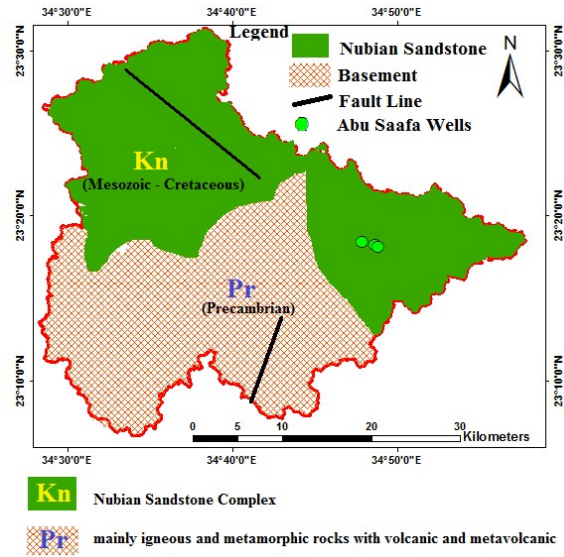


Fig. 4: Aquifer distribution in the study area

Unconformable and/or structurally controlled connections between Pre-Cambrian basement rocks and Cretaceous sandstone, as well as between Quaternary deposits and Cretaceous sandstone outcrops, support the concept that these three aquifers are hydraulically connected.

MATERIALS AND METHODS

1. Flood Conditioning Factors (FCFs)

Many studies have used remote sensing data to assess and forecast flood risk, including climatic conditions, geomorphic and physical watershed parameters, soil characteristics, and land use/cover (Hong and Abdelkareem, 2022). Considering an analysis of the literature and its importance to flood susceptibility, nine flood conditioning factors were selected to collect pertinent data and avoid unnecessary complexity in spatial modeling at the national level: Elevation, slope, flow accumulation, rainfall intensity, distance from drainage, TWI (Topographic Wetness Index), LULC (Land Use/Land Cover), and NDVI (Normalized Difference Vegetation Index) are some of the factors that affect drainage network density. For this study, many layers are prepared, including maps of elevation, slope, flow accumulation, distance from drainage, drainage network density, and TWI and LULC. Table 1 reports the original data and their sources that have been applied to analyze flood conditioning factors.

Table (1) Data sources used for processing of flood conditioning factors

| Data | Source |
|----------|--|
| DEM | ALOS PALSAR DEM data was available in Alaska Satellite Facility (ASF) 12.5m High resolution terrain corrected DEM data (https://search.asf.alaska.edu/) |
| LULC | Global land use/land cover map (LULC) at 10m resolution created from ESA Sentinel-2 imagery (2022) (https://livingatlas.arcgis.com/landcoverexplorer/#mapCenter=3) |
| NDVI | Landsat 8 images (OLI/TIRS) imagery (https://ers.cr.usgs.gov/) using |
| Rainfall | Climatic Research Unit (University of East Anglia) and Met Office, CRU TS Version 4.07 (https://crudata.uea.ac.uk/cru/data/hrg/cru_ts_4.07/) |

1.1. Analytical Hierarchy Process (AHP)

To assess the influence of individual Flood Conditioning Factors (FCFs) on flood susceptibility, the FCFs were correlated in pairs of two by two on the flood susceptible zone. The appropriate steps to set up the analytical hierarchy process approach in the Wadi Abu Safaa are outlined below (Saaty, 2008) (Figure 5):

Step 1: Assigning a relative significance of a value ranging from 1 to 9 to each factor to generate a pair-wise comparison matrix. The value of one suggests that the two factors under consideration are of the same significance. On the other hand, a value of 9 shows that the row factor seems significantly more than the column factor (Table 2).

Step 2: Prepare the normalized pair-wise comparison matrix table by dividing each value in a column by the sum of a column (Table3)

Step 3: The normalized pair-wise comparison matrix table's sum of each row can be divided by the total number of criteria or sum of each row can be divided by the total number of criteria or factors to determine the criterion weight (W_i) for each criterion or factor. (Table 5).

Step 4: The Weighted Sum Value (WSV) concept is used to assess if the estimates are identical. WSV is calculated by multiplying each criterion by the associated criterion weight, then adding each row (Table 5).

Step 5: Determine the ratio of WSV to W_i for every factor (Table 5).

Step 6: In order to ascertain the accuracy and consistency of the comparison, the consistency index (CI) is calculated as follows: $\lambda_{max} - n / (n - 1)$, where λ_{max} denotes the n-order matrix's greatest eigenvalue. Additionally, it signifies the mean proportion of WSV to W_i , with n representing the number of factors (Table 5).

Step 7: Calculate the consistency proportion specified in the following equation: $CR = CI / RI$, where CR stands for consistency ratio, CI for consistency index, and RI stands for random index, which fluctuates according to the number of elements in the pairwise matrix (Table 5). When the CR declines below 0.10, the pairwise comparison matrix has feasible consistency. Otherwise, if the CR is greater than or equal to 0.10, it shows that the pairwise comparison has unacceptable consistency, and the comparison procedure must be repeated until the value of the CR reaches below 0.10. (Table 4) illustrates various RI values.

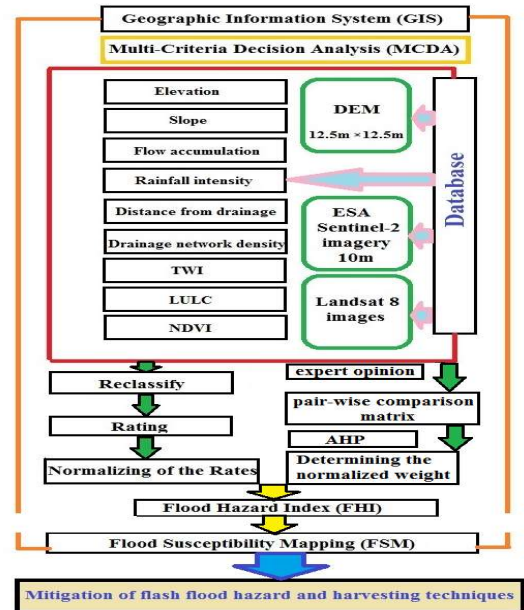


Fig. 5: Schematic illustration of the application of hydrological and AHP modeling into GIS.

Table (2) Pairwise comparison matrix of flood influencing factors for AHP

| Factor | Elevation | Slope | Flow accumulation | Rainfall intensity | Distance from drainage | Drainage network density | TWI | LULC | NDVI |
|--------------------------|-----------|-------|-------------------|--------------------|------------------------|--------------------------|-------|-------|------|
| Elevation | 1 | 2 | 2 | 2 | 2 | 3 | 3 | 2 | 4 |
| Slope | 0.5 | 1 | 1 | 3 | 2 | 3 | 3 | 1 | 5 |
| Flow accumulation | 0.5 | 1 | 1 | 2 | 2 | 3 | 3 | 2 | 4 |
| Rainfall intensity | 0.5 | 0.33 | 0.5 | 1 | 2 | 2 | 3 | 2 | 4 |
| Distance from drainage | 0.5 | 0.5 | 0.5 | 0.5 | 1 | 2 | 3 | 3 | 4 |
| Drainage network density | 0.33 | 0.33 | 0.33 | 0.5 | 0.5 | 1 | 2 | 2 | 4 |
| TWI | 0.33 | 0.33 | 0.33 | 0.33 | 0.33 | 0.5 | 1 | 1 | 3 |
| LULC | 0.5 | 1 | 0.5 | 0.5 | 0.33 | 0.5 | 1 | 1 | 3 |
| NDVI | 0.25 | 0.2 | 0.25 | 0.25 | 0.25 | 0.25 | 0.33 | 0.33 | 1 |
| Sum | 4.42 | 6.70 | 6.42 | 10.08 | 10.42 | 15.25 | 19.33 | 14.33 | 32 |

Because CR = 0.05 is below the limit (0.1), the weights' consistency is constant. The nine chosen elements are arranged linearly, with their weights computed beforehand. An equation was used to calculate the flood risk index.

$$FHI = \sum_{i=1}^n (w_i \times X_i)$$

At every point, X_i represents the factor classification, W_i represents the weight of individual criteria, and (n) represents the number of elements.

Table (3) Normalized weights determined for each flood factor

| Factor | Elevation | Slope | Flow accumulation | Rainfall intensity | Distance from drainage | Drainage network density | TWI | LULC | NDVI | Weight |
|--------------------------|-----------|-------|-------------------|--------------------|------------------------|--------------------------|------|------|------------|--------|
| Elevation | 0.23 | 0.30 | 0.31 | 0.20 | 0.19 | 0.20 | 0.16 | 0.14 | 0.13 | 1.84 |
| Slope | 0.11 | 0.15 | 0.16 | 0.30 | 0.19 | 0.20 | 0.16 | 0.07 | 0.16 | 1.49 |
| Flow accumulation | 0.11 | 0.15 | 0.16 | 0.20 | 0.19 | 0.20 | 0.16 | 0.14 | 0.13 | 1.43 |
| Rainfall intensity | 0.11 | 0.05 | 0.08 | 0.10 | 0.19 | 0.13 | 0.16 | 0.14 | 0.13 | 1.08 |
| Distance from drainage | 0.11 | 0.07 | 0.08 | 0.05 | 0.10 | 0.13 | 0.16 | 0.21 | 0.13 | 1.03 |
| Drainage network density | 0.08 | 0.05 | 0.05 | 0.05 | 0.05 | 0.07 | 0.10 | 0.14 | 0.13 | 0.71 |
| TWI | 0.08 | 0.05 | 0.05 | 0.03 | 0.03 | 0.03 | 0.05 | 0.07 | 0.09 | 0.49 |
| LULC | 0.11 | 0.15 | 0.08 | 0.05 | 0.03 | 0.03 | 0.05 | 0.07 | 0.09 | 0.67 |
| NDVI | 0.06 | 0.03 | 0.04 | 0.02 | 0.02 | 0.02 | 0.02 | 0.02 | 0.03 | 0.26 |
| | | | | | | | | | Sum | 9 |

Table (4) Random Index for the number of element/criteria

| n | 3 | 4 | 5 | 6 | 7 | 8 | 9 | 10 | 11 | 12 | 13 | 14 | 15 |
|----|------|------|------|------|------|-----|------|------|------|------|------|------|------|
| RI | 0.52 | 0.89 | 1.11 | 1.25 | 1.35 | 1.4 | 1.45 | 1.49 | 1.51 | 1.54 | 1.56 | 1.57 | 1.58 |

The Flood Hazard Index (FHI) was applied in the Abu Safaa Wadi catchment using the following equation (Table 6): $FHI = [0.204 \times (\text{Elevation})] + [0.166 \times (\text{Slope})] + [0.159 \times (\text{Flow accumulation})] +$

Mitigation of Flash Flood Hazards Through the Optimum Utilization of Surface Water Harvesting Techniques of Wadi Abu Safaa, Northwest of El Shalateen Area, Red Sea, Eastern Desert, Egypt

$[0.120 \times (\text{Rainfall})] + [0.114 \times (\text{Distance from drainage})] + [0.079 \times (\text{Drainage Density})] + [0.054 \times (\text{TWI}) + [0.074 \times (\text{LULC}) + [0.029 \times (\text{NDVI})]$. As demonstrated in this basin case study, the Flood Hazard Index (FHI) (Table 6) model appears to act as a significant modeling tool for an initial plan for the mapping of flood zones. As a result, it has been feasible to identify the regions subjected to flood hazards through Flood Susceptibility Mapping (FSM) in the Abu Safaa Wadi watershed utilizing the Flood Hazard Index multi-criteria decision analysis (FHI-MCDA) method. These areas must be addressed in future land-use plans.

Table (5) Calculation of consistency, λ_{\max} : maximum value of the comparison matrix, RI: Random indices, CR: consistency ratio.

| Factor | Weighted Sum Value (WSV) | Criterion Weight (Wi) | Weight % | WSV/Wi | λ_{\max} | CI | CR |
|--------------------------|--------------------------|-----------------------|------------|--------------------|------------------|------------------|------|
| Elevation | 1.99 | 0.204 | 20.4 | 9.70 | | | |
| Slope | 1.64 | 0.166 | 16.6 | 9.91 | | | |
| Flow accumulation | 1.56 | 0.159 | 15.9 | 9.86 | | | |
| Rainfall intensity | 1.17 | 0.120 | 12.0 | 9.75 | 9.61 | 0.08 | 0.05 |
| Distance from drainage | 1.1 | 0.114 | 11.4 | 9.59 | | | |
| Drainage network density | 0.75 | 0.079 | 7.9 | 9.49 | | | |
| TWI | 0.51 | 0.054 | 5.4 | 9.36 | | | |
| LULC | 0.7 | 0.074 | 7.4 | 9.41 | | | |
| NDVI | 0.27 | 0.029 | 2.9 | 9.41 | | | |
| n = 9 | | 1 | 100 | Sum = 86.48 | | RI = 1.45 | |

2. Watershed Delineation

The different indicators of drainage morphometry (drainage network) give inferences regarding hydrologic and geologic aspects of the catchment. Given that the primary goal of the paper is to evaluate the susceptibility to flood risks of the Abu Safaa catchment and flood prevention and mitigation, The eight morphometric characteristics that impact rainwater harvesting (RWH) sites were extracted using ArcGIS 10.8, Watershed Area (A), Basin Slope, Length of Overland Flow (Lo), Maximum Flow Distance (MFD), Basin Length (Lb), Drainage Density (Dd), Infiltration Number (FN), and Volume of Annual Flood (VAF).

Table (6) Thematic map weights for generating FHI for Wadi Abu Safaa

| Thematic Layer | Normalized Layer Weight (Wi) | Detailed Features/Sub-Classes | Flood Susceptibility | Rank | Area (%) |
|---|------------------------------|-------------------------------|----------------------|------|----------|
| Elevation (m) | 0.204 | 219 – 349 | Very high | 5 | 7.93 |
| | | 350 – 450 | High | 4 | 19.73 |
| | | 451 – 532 | Moderate | 3 | 39.19 |
| | | 533 – 635 | Low | 2 | 26.47 |
| | | 636 - 1,050 | Very low | 1 | 6.66 |
| Slope (degree) | 0.166 | 0-15 | Very high | 5 | 71.26 |
| | | 15-30 | High | 4 | 23.71 |
| | | 30-45 | Moderate | 3 | 4.65 |
| | | 45-60 | Low | 2 | 0.33 |
| | | 60-79 | Very low | 1 | 0.02 |
| Flow accumulation (pixels) | 0.159 | 0 - 200,000 | Very low | 1 | 99.80 |
| | | 200,000 - 1,500,000 | Low | 2 | 0.12 |
| | | 1,500,000 - 3,500,000 | Moderate | 3 | 0.03 |
| | | 3,500,000 - 6,000,000 | High | 4 | 0.00 |
| | | 6,000,000 - 11,900,000 | Very high | 5 | 0.02 |
| Rainfall intensity (mm/year) | 0.120 | 15-15.3 | Very low | 1 | 6.15 |
| | | 15.3-15.6 | Low | 2 | 7.89 |
| | | 15.6-15.9 | Moderate | 3 | 12.46 |
| | | 15.9-16.1 | High | 4 | 19.52 |
| | | 16.1-16.4 | Very high | 5 | 53.99 |
| Distance from drainage (m) | 0.114 | 0-33 | Very high | 5 | 0.00 |
| | | 33-100 | High | 4 | 0.53 |
| | | 100-300 | Moderate | 3 | 39.54 |
| | | 300-500 | Low | 2 | 37.20 |
| | | 500-602 | Very low | 1 | 22.70 |
| Drainage network Density (m/km ²) | 0.079 | 0-2 | Very low | 1 | 1.14 |
| | | 2-5 | Low | 2 | 29.35 |
| | | 5-7 | Moderate | 3 | 40.96 |
| | | 7-9 | High | 4 | 22.06 |
| | | 9-11.8 | Very high | 5 | 6.34 |
| TWI | 0.054 | <5 | Very low | 1 | 24.07 |
| | | 5-7 | Low | 2 | 38.49 |
| | | 7-9 | Moderate | 3 | 25.90 |
| | | 9-23 | High | 4 | 11.53 |
| | | 23-26 | Very high | 5 | 0.01 |
| LULC (Pixels) | 0.074 | Water | Very high | 5 | 0.00 |
| | | Flooded vegetation | High | 4 | 0.05 |
| | | Crops | Moderate | 3 | 1.65 |
| | | Bare ground | Low | 2 | 9.64 |
| | | Rangeland | Very low | 1 | 88.65 |
| NDVI | 0.029 | 0.005-0.06 | Very high | 5 | 20.72 |
| | | 0.06-0.07 | High | 4 | 37.01 |
| | | 0.07-0.08 | Moderate | 3 | 29.27 |
| | | 0.08-0.09 | Low | 2 | 9.72 |
| | | 0.09-0.31 | Very low | 1 | 3.28 |

Table (7) Morphometric parameters of a river basin

| No. | Morphometric Parameters | Formula | Reference |
|-----|------------------------------|------------------------------|----------------|
| 1 | Watershed Area (A) | GIS software Analysis | |
| 2 | Basin length (Lb) | GIS software Analysis | |
| 3 | Maximum flow distance (MFD) | GIS software Analysis | |
| 4 | Basin Slope | DEM in GIS software Analysis | |
| 5 | Drainage Density (Dd) | $Dd=Lu/A$ | Horton (1945) |
| 6 | Infiltration Number (FN) | $FN = Dd*Fs$ | Faniran (1968) |
| 7 | Length of overland flow (Lo) | $Lo=1/Dd*2$ | Horton (1945) |
| 8 | Volume of annual flood (VAF) | SCS method | |

3. Estimation of rainfall/surface runoff relationship

Generally, desert floods are characterized by sharp peak discharges with short durations. Systems with high rainfall and longevity can relieve drought in the places they move through. Unlike flash floods, flooding lasts longer—it may continue for days or even weeks. As a result, a flood brought on by high or extreme rainfall in a short time, usually less than six hours and frequently within 3 hours (NWS, National Weather Surface 2023). Accordingly, medium- to long durations of severe flash floods battered the study area several times over the last decade. Such characteristics are used to evaluate the risk of floods and design river regulation structures. The rainfall data is collected from the website for satellite data (GSMAP, Jaxa Global Rainfall Watch 2023). These data were used to create hydrographs of the Abu Safaa watershed. The Soil Conservation Service (SCS-CN) technique (SCS, 1972) was applied to estimate the rainfall/runoff relationship of the Abu Safaa basin. The SCS runoff curve number approach is employed for analyzing the hydrographs at each sub-catchment outlet, connecting hydrograph elements (lag time, peak discharge, base time, etc.) to catchment characteristics (area, length, hydrological characteristics, soil cover types). Depending on the hydrological soil group and hydrologic conditions, the CN ranges from 0 to 100. The hydrological software “HEC-HMS” version 4.11 is implemented to simulate the hydrological situation of the investigated basin and develop the basin hydrograph (HEC-HMS 2023). The model input data contains rainfall data and physical watershed aspects (basins, subbasins, areas, reaches, and outlets) (Chow et al., 1988). Hydrological parameters, i.e., initial abstractions (Ia), curve number (CN), slope, impervious ratio, time of concentration Tc (Kirpich, 1940), and time lag (TL), The HEC-HMS model, routed with the Muskingum method, is the final phase in generating the Abu Safaa basin hydrograph. Routing is the process of moving runoff from the various watershed outlets downstream along the stream and eventually to the overall watershed system's outlet or sink.

RESULTS

1. Factors Influencing Flash Flood Hazards

1.1. Elevation

Elevation is a typical measure for describing regions susceptible to flash floods (FFHs). Lower elevation areas are more likely to experience flash floods due to high rainfall accumulation in lowland areas and the fact that water moves more quickly from high elevation to low elevation (Waqas et al., 2021) than higher elevation areas. Then, using DEM data, an elevation map was classified into five categories: very high, high, moderate, low, and very low. Table 6 and Figure 6a. Flooding is more likely at low elevations (450m) than at high elevations (> 533m).

1.2. Slope

The slope is the most important index for identifying and describing surface runoff and liable area for FFHs, since it indicates elevation variation and has a direct influence on catchments, runoff speed, and infiltration capacities (Ikirri et al., 2022). Runoff speed corresponds to the slope's impact on the occurrence of destructive floods. Groundwater prospects are favorable in comparison to the low-slope region. According to Demek's (1972) slope model (Table 6), the slope classes were defined. Low-slope areas are concentrated in the Abu Safaa basin's downstream sector, whereas high-slope areas are emphasized in the mountainous regions to the basin's west and south (Fig. 6b).

1.3. Flow accumulation

It depicts the total flow of water from cells upstream to a certain cell. High flow accumulation factor values indicate concentrated flow locations, which increases the potential risk of floods. This factor ranges from 0 to 11,900,000, with the highest values observed in the flow of Wadi Abu Safaa's main tributaries (Table 6 and Figure 6c).

1.4. Rainfall

Rainfall serves as the primary source of runoff over the ground's surface, resulting in lowland floods. According to Nyarko (2002), rainfall is directly associated with flash flood hazards (FFHs) and plays a major role in the risk of severe floods, which are produced by heavy rainfall over a short period of time. Runoff occurs when rainfall intensity exceeds the soil's infiltration capacity. Rainfall is the essential source of replenishment for groundwater aquifers. The Wadi Abu Safaa rainfall intensity map, which ranges from 15 to 16.4 mm/year, is classified into five categories. Specifically, very low, low, moderate, high, and extremely high (Table 6, Figure 6d). Precipitation is most common at the highest elevations in the western part, such as G. Amerit, G. Aqab El-Nogoom, and G. Shyanite, but it decreases downstream (Figure 1).

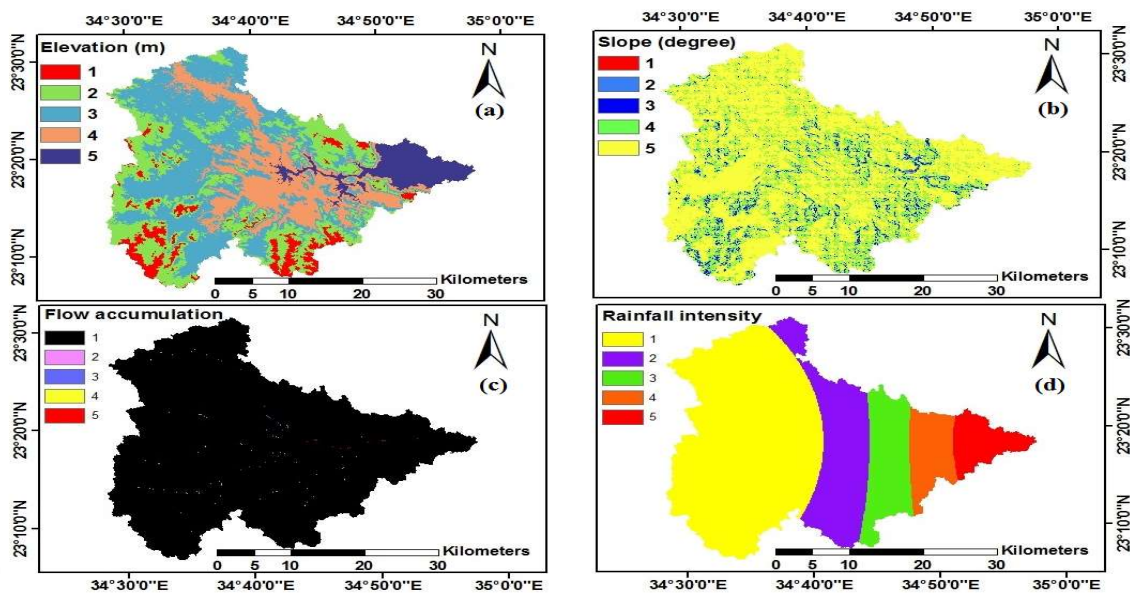


Fig. 6: Flood conditioning factors: a) Elevation, b) Slope, c) Flow accumulation, d) Rainfall intensity

1.5. Distance from drainage

Because areas adjacent to drainage systems are more vulnerable to flooding, distance from drainage is a significant and crucial element in minimizing or exacerbating flood occurrences. As the places closest to the river system are impacted, the hazard decreases with increasing distance. In the Abu Safaa watershed, 40% of the studied area is less than 300 m, making it moderately vulnerable to flooding, while the rest (i.e., 60%, 300–602 m) is lowly vulnerable to flooding (Table 6, Figure 7a).

1.6. Drainage Density

Drainage density is the measure that is relative to water accumulation pathways, resulting in an increase in the amount of water in tributaries and the occurrence of floods. Higher drainage density

increases susceptibility to floods and surface runoff while decreasing permeability (Sharma et al., 2021). The drainage density in the Wadi Abu Safaa watershed ranges from 0 to 11.8 m/km² (Table 6, Figure 7b).

1.7. Topographic Wetness Index (TWI)

TWI is a widely used hydraulic modeling metric that measures a region's ability to absorb water and is often used to examine the topographical effect on hydrological processes. It also corresponds to the amount of flow accumulation at a certain place in the watershed as well as the propensity of water flow downslope due to gravity, which increases water flow accumulation and, therefore, its damaging capacity. TWI is beneficial to FFHs because high TWI values indicate increased flood risk and low TWI values suggest decreased flood vulnerability (Ullah and Zhang, 2020). TWI with (> 9) is associated with a higher risk in this study, whereas TWI with (7) is associated with a lower risk (Table 6, Figure 7c).

1.8. Land use/Land cover

Land use and land cover (LULC) are essential in the flooding process as they influence several hydrological operations such as permeability, evapotranspiration, and runoff. Water, Flooded Vegetation, Crops., Bare Ground, and Rangeland are the five classes of the generated LU/LC map (Table 6, Figure 7d).

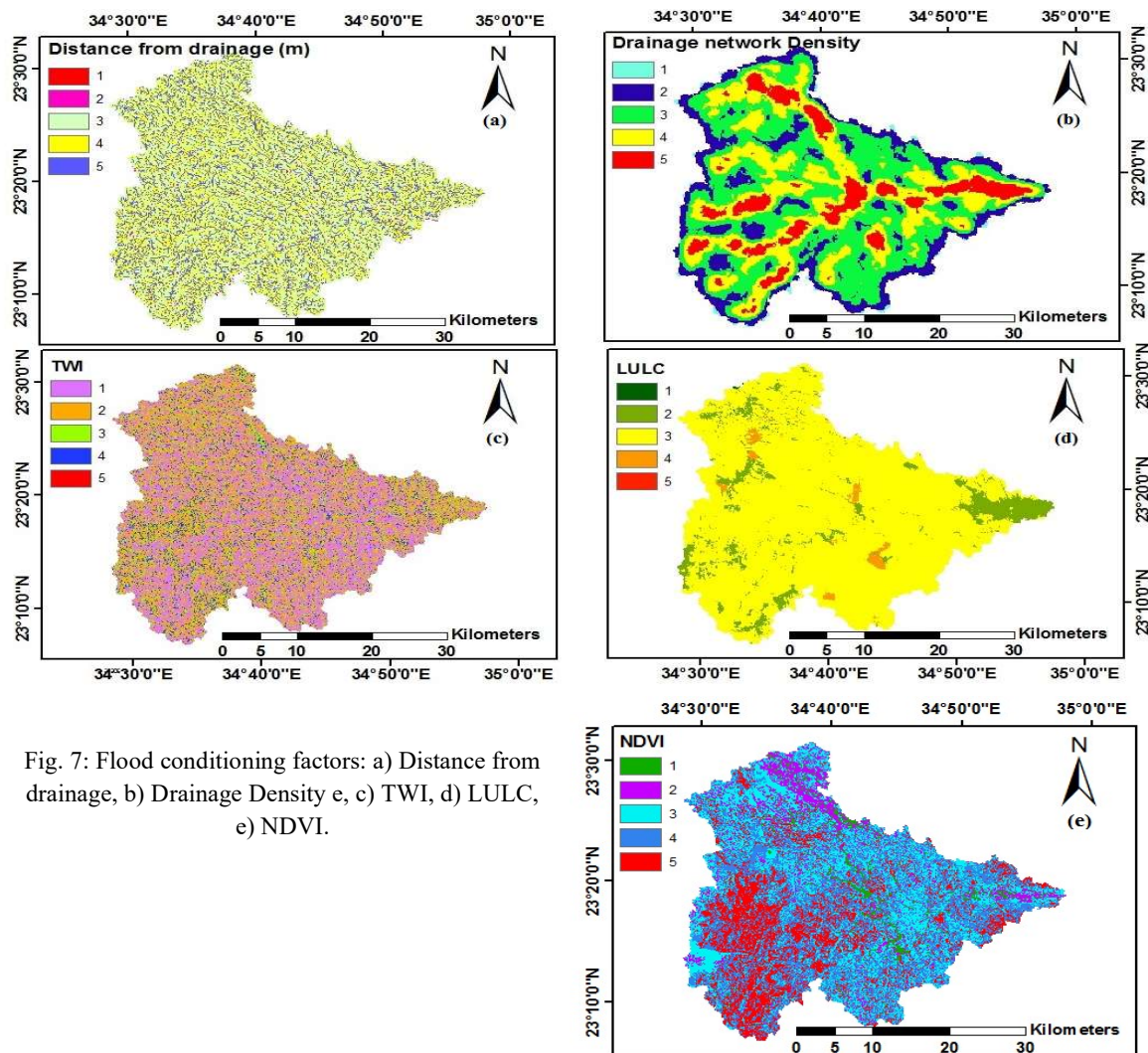


Fig. 7: Flood conditioning factors: a) Distance from drainage, b) Drainage Density, c) TWI, d) LULC, e) NDVI.

1.9. Normalized Difference Vegetation Index (NDVI)

The normalized differential vegetation index (NDVI) is often used to assess vegetation as a flood defense element since it slows runoff and acts as a barrier (Tehrany et al., 2014). The NDVI scale runs from -1 to +1, since great values indicate healthy vegetation cover, whereas smaller values indicate sparse vegetation. NDVI map of Wadi Abu Safaa, which ranges from 0.005 to 0.31. Ninety-seven percent (97%) has a lower NDVI value, indicating the presence of sparse vegetation (Table 6, Figure 7e).

2. Flood Susceptibility Map

The final FSM was generated using the AHP method by integrating nine (9) factors and classified into five flood potentiality levels extending from very low to very high. Accordingly, we discover that 11.21% of the study region is accounted for by the very low class, 26.5% by the low class, 32.81% by the moderate class, 20.18% by the high class, and 9.3% by the very high class (Figure 8). Elevation, slope, flow accumulation, rainfall intensity, and distance from drainage (Figs. 6a, 6b, 6c, 6d, and 7a) were given high weights in this analysis. The relative impact of the remaining conditioning elements used in this study (drainage density, TWI, LULC, and NDVI) is not visible. These criteria have the smallest weights and have no significant impact. It is also worth noting that elevation and slope degree were designated the utmost relative significance, showing that slope is the most valuable conditioning element for identifying flood-prone sectors. Areas of very high potentiality appear to occupy a surface area of 111.97 km², which is the smallest part of the study region. These flood-prone areas have generally exhibited a combination of very low elevation, a low degree of slope, and a high drainage density. The study's findings indicate that flood-vulnerable areas extend eastwards from the main Abu Safaa catchment, with the affected areas situated in the downstream of the basin (Figure 8). Using the data from past historical occurrences to compare with the established Flood Hazard Index (FHI) model proves that the model is reliable. Because historical flood events recorded in the last few years show the convergence of flood-prone areas in the downstream (i.e., eastern) part of the Abu Safaa watershed, the AHP methodology has proven its effectiveness in that regard. As a result, these findings provide baseline data that must be considered during flood prevention and mitigation strategies.

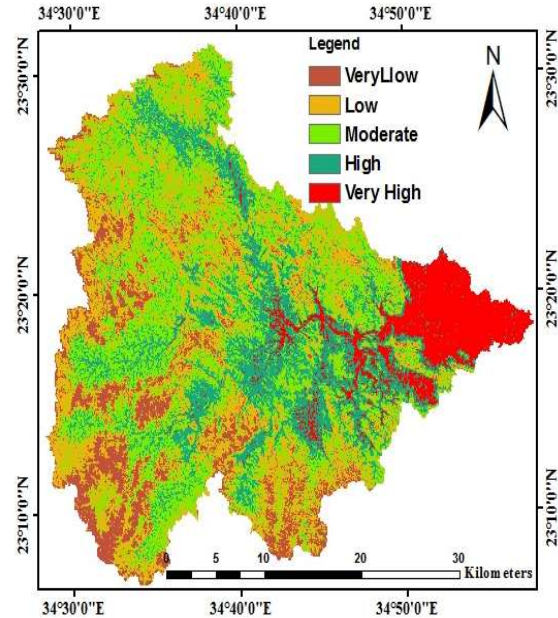


Fig. 8: Flood susceptibility Map (FSM) of Wadi Abu Safaa Watershed

3. River basin morphometry runoff calculations

3.1. Watershed Area (A)

The catchment area is recognized as the most significant morphometric component influencing the total runoff volume (Table 8). The larger the basin's area, the higher the cumulative runoff volume.

Table (8) Selected morphometric aspects of Wadi Abu Safaa basin

| Aspect | Units | | |
|------------------------------|-----------------------|------------|----------------|
| Watershed Area (A) | (km ²) | 1203.7 | |
| Basin length (Lb) | (km) | 48.11 | |
| Maximum flow distance (MFD) | (km) | 59.44 | |
| Basin Slope | (degree) | 0-15 | Gentle |
| | | 15-30 | Moderate |
| | | 30-45 | Moderate Steep |
| | | 45-60 | Steep |
| | | 60-79 | Very Steep |
| Drainage Density (Dd) | (km/km ²) | 3.15 | |
| Infiltration Number (FN) | (km ⁻³) | 23.36 | |
| Length of overland flow (Lo) | (km) | 0.1 | |
| Volume of annual flood (VAF) | | SCS method | |

3.2. Basin length (Lb)

Lb is defined as the distance separating two similar parts of the watershed. The Lb value of the Abu Safaa catchment is 48.11 (Table 8), which falls under the long basin length and relatively high potentiality of RWH.

3.3. Maximum flow distance (MFD)

The maximum flow path for water within a drainage basin is measured in kilometers. The greater the MFD, the larger the possibility for RWH. The MFD value of the Abu Safaa basin is 59.44, i.e., moderate RWH potential (Table 8).

3.4. Basin Slope (degree)

Slope is a fundamental element that directly impacts the runoff and infiltration of any ground. The research region's slope map was divided into five-degree classes: 0–15° (gentle), 15–30° (moderate), 30–45° (moderate steep), 45–60° (steep), and 60–79° (very steep) (Table 6, Figure 6c). Gentle slopes were reflected in 71.26% of the Wadi Abu Safaa basin area and were rated "excellent" for handling groundwater due to the nearly flat topography being the most suitable for infiltration, i.e., high potentiality for RWH. Because of the slightly undulating topography that maximizes percolation, moderate slopes are also classified as good zones. the steep class with very little infiltration and high surface runoff.

3.5. Drainage Density (Dd)

Horton (1945) defines drainage density (Dd) as the proportion of all stream lengths to the basin's per-unit area. Research has shown that high relief, sparse vegetation, and impervious surface materials cause mountain nature to have a high drainage density (Dd), while low relief and high percolation cause plateau environments to have a low Dd. Wadi Abu Safaa basin's overall drainage density is 3.15 km/km², indicating high drainage densities (Table 8). As a result, increased runoff combined with increased flow velocity increases the basin's potential for downstream flooding, or RWH.

3.6. Infiltration Number (FN)

It implies impervious rock and higher relief; thus, the greater the infiltration number, the smaller the infiltration, resulting in high hazardous surface runoff. The Wadi Abu Safaa basin has a FN value of 23.36 (Table 8), indicating a high infiltration number and a high potential RWH.

3.7. Length of overland flow (Lo)

The flow of water on the land surface towards its confluence, also known as the outlet, is measured by the Overland Flow (Lo) value, which is inversely correlated with the watershed's drainage density. The longer the runoff's travel time, the lower the Lo value. The study basin's values of Lo are 0.1 (Table 8), indicating low RWH potentiality and the fastest overland flow that has been observed.

3.8. Volume of annual flood (VAF)

The SCS-CN approach was utilized to predict the rainfall/runoff relationship across the Abu Safaa basin (Table 9). The accurate determination of the curve number (CN) value represents the primarily essential parameter in this method. The hydrological soil group (A) CN value (Table 9) was obtained, and the estimated weighted CN value is 73.4. As a result, Abu Safaa's initial abstraction (Ia) is 18.41mm.

The maximum monthly precipitation for a 98-year period (base period 1925–2023, GSMAP, 2023) (Fig. 9) was approximately 51.28 mm on February 15–16, 2018, during a 39-hour period (i.e., from 3 p.m. to 6 a.m.), severely damaging the study area's infrastructure. This heavy storm is chosen for analysis to compute the runoff that occurs as a result. The hyetograph of this storm is shown in Fig. 10.

Table (9) Rainfall/runoff relationship and results using SCS-CN method in Abu Safaa

| Area km ² | Soil type | Weighted CN | S (mm) | Ia (mm) | Rainfall/runoff relation Q (mm) |
|----------------------|-----------|-------------|--------|---------|---------------------------------|
| 1203.7 | A | 73.4 | 92.05 | 18.41 | $Q=(P-18.41)^2/P+73.64$ |

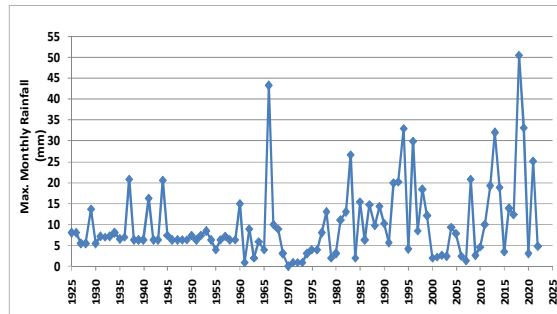


Fig. 9: Relation between maximum monthly rainfall (mm) and the corresponding year

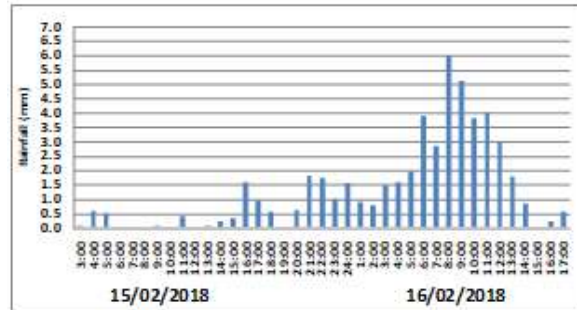


Fig. 10: Hyetograph of the selected rainfall storm (February 2018)

The runoff volume of the ungauged Abu Safaa basin was estimated applying the HEC-HMS modeling software (V. 4.11), that was developed to model the basin's rainfall and runoff processes. The time of concentration (Tc) was estimated to be 376.7 minutes, and the latency time (TL) was 226 minutes (Table 10). The outcome parameters of the HEC-HMS program involve the hydrograph at the catchment outlet, loss rates, flood peak, and surplus water volume of the Abu Safaa basin (Figure 11).

Table (10) Main inputs in HEC-HMS domain of Wadi Abu Safaa.

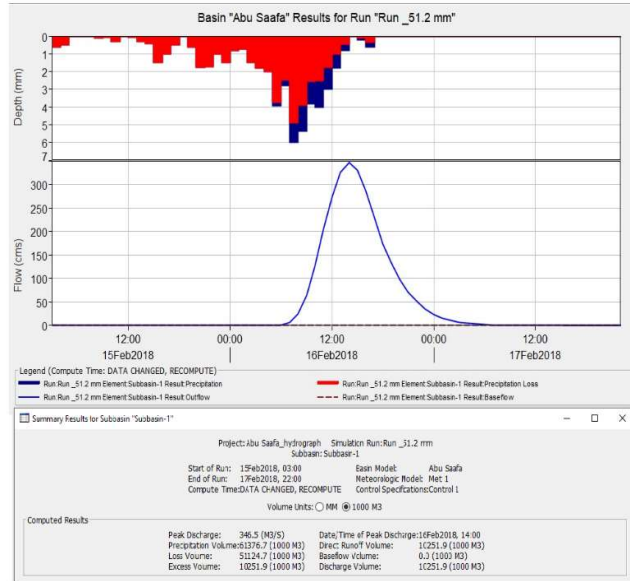
| Basin name | Weighted CN | Losses (mm) | Ia | Tc (min) | (TL) (min) | Precipitation (mm) | Method |
|------------|-------------|-------------|----|----------|------------|--------------------|--------|
| Abu Safaa | 73.4 | 18.41 | | 376.7 | 226 | 51.28 | SCS-CN |

The results show that in response to the studied storm event (February 2018), the un-gauged Abu Safaa basin received a total of 61.4×10^6 m³ of rainfall, resulting in a water harvesting potential of approximately 10.3×10^6 m³. The majority of this water fell out during the February 2018 storm, which spanned around

39 hours with a maximum intensity of 5 mm and a rain depth of 51.2 mm. The Abu Safaa basin has a peak discharge of 346.5 m³/s. The study basin's total loss is projected to be 51.1 × 10⁶ m³.

4. Water Harvesting and Flashflood Mitigation

Due to its high risk of flooding, the Abu Safaa wadi watershed needs special attention. This is especially important in areas where the Bedouin community lives, agriculture, various development projects (such as mining, tourism, etc.), and infrastructure are concerned to prevent disasters brought on by these extreme events. A multi-criteria decision analysis (MCDA) via the Analytical Hierarchy Process (AHP) method, which relies on a variety of conditioning variables that reflect the physical features of the region under investigation, is combined with the Geographic Information System (GIS) to create flash flood hazard zones (FFHs) in the Abu Safaa wadi. These parameters were utilized to create a weighted spatial probability model that identified possible rainwater harvesting sites. The water harvesting scheme's location and technique were determined using the MCDA, followed by a physical analysis (geology, slope (%), soil). Furthermore, according to the standards established by the UN Food and Agriculture Organization (FAO), socioeconomic aspects must be regarded as a main element in the selection of rainwater harvesting (RWH) locations. As a result, RWH structure sites will be chosen based on the following: a) To meet water needs, structures should be located near Bedouin local residences, agriculture, and various development projects. b) Structures will be chosen to be located along active streams to provide adequate runoff water collection. Accordingly, the recommended rainwater collection technique for the watershed may include check dams, wadi-bed cultivation, jessour, percolation ponds, and cisterns. As anticipated, water harvesting could simultaneously mitigate the risk of flash floods downstream by impounding water in designated areas and providing an additional conventional water source. Building a flood control dam will be a prudent way to reduce the influence of these floods, which originate at the inlet catchment's level, on the development plan for this basin. Figure 12 illustrates the appropriate sites for surface water storage, replenishment of groundwater, and/or combined usage to mitigate floods. By lengthening the hydrographic basins' concentration period and lowering the flood peak, water harvesting structures lower the water velocity during flash floods (Colombo et al., 2002). When water is stored and infiltrated in a watershed, it has the potential to reduce runoff. Increasing the surface layer's storage capacity can also reduce the probability of flash floods. Consequentially, the suggested technique for building structures that capture water may prevent damaging flash floods by decreasing water velocity through flash flood episodes and providing a strong supply of surface water to meet the requirements of groundwater recharge in the Quaternary aquifer and the exposed Nubian Sandstone aquifer, which are heavily used by the area's farmers.



CONCLUSIONS AND RECOMMENDATIONS

Flood Susceptibility Mapping (FSM) in the Abu Safaa basin using the Flood Hazard Index (FHI) multi-criteria analysis method has enabled the delimitation of flood-prone regions, which must be considered in sustainable land-use planning. Over 60% of the basin's surface is very sensitive to flooding, particularly in the basin's downstream portion. The elevation has the greatest impact on these floods, followed by slope, flow accumulation, rainfall intensity, and distance from drainage; finally, we should disregard the impact of drainage density, TWI, LULC, and NDVI, which are assigned the smallest weights and have no significant impact. The Flood Hazard Index (FHI) simulates flooding thresholds that match past historical occurrences documented in the research region, demonstrating the model's validity. As shown in this watershed case research, the Flood Hazard Index (FHI) model provides an effective tool for a preliminary approach to mapping flash flood hazard zones (FFHs) applying the Analytical Hierarchy Process (AHP) despite the absence of hydrometric data. Moreover, the SCS-CN approach was used to assess the rainfall/runoff relationship throughout the Abu Safaa watershed. The runoff volume of the ungauged Abu Safaa basin was calculated by hydrograph creation using the HEC-HMS modeling program (V. 4.11). Accordingly, Abu Safaa basin received a total of $61.4 \times 10^6 \text{ m}^3$ of rainfall (15–16 February 2018), which led to a water harvesting potential of about $10.3 \times 10^6 \text{ m}^3$ and total losses of about $51.1 \times 10^6 \text{ m}^3$. The model's application results allowed us to suggest ways to mitigate the effects of these floods. In this instance, the locations of rainwater harvesting (RWH) structures will be chosen in various basin zones; upstream, a capping dam and Jessour system will be built to delay water flow and enable it to gradually infiltrate downstream to Quaternary deposits; downstream, wadi-bed cultivation, percolation ponds, and sterns will be built in the scattered outcrops of fluviatile Nubian sandstone to collect rainwater for domestic and agricultural purposes. Finally, the strategy for analyzing and mitigating flood susceptibility on a local scale that has been presented can offer a good substitute for the evaluation of the initial flood hazard and the determination of possibly severe flood risk in the Abu Safaa basin, which ought to be updated for at least ten years.

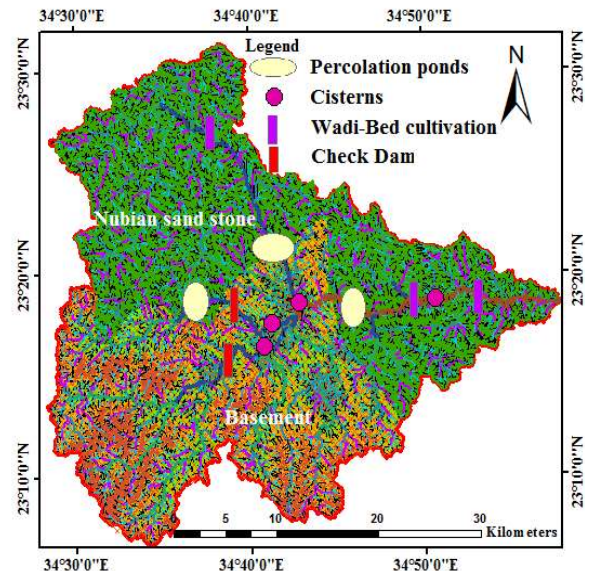


Fig. 12: Sites of water harvesting techniques and mitigation suggested for possible implementation in Wadi Abu Safaa

REFERENCES

- Al-Zu'bi, M., Dejene, S.W., Hounkpè, J., Kupika, O.L., H., Lwasa, S., Mbenge, M., Mwongera, C., Ouedraogo, N.S., Touré, N.E., 2022.** African perspectives on climate change research. *Nature Climate Change*, 12, 1078-1084.
- Awad, A., Abd El-Aal, E., and Khashaba A.A., 2021.** Phases of Magmatic Activities in South Wadi Hodein-Shalatein, Egypt: Resolving controversy about their age using Paleomagnetism and AMS. *Nriag Journal OF Astronomy and Geophysics*. 11, 1, 21-32.
- Chow, V.T., Maidment, D.R., and Mays, L.W., 1988.** In *Applied Hydrology*, McGraw-Hill, New York, U.S.A.

- Colombo, A., Hervás Javier, G., and Arellano, Ana Lisa Vetere, 2002.** Guidelines on Flash Flood Prevention and Mitigation. Nadies Project, European Commission (EU) Joint Research Centre Institute for the Protection and Security of the Citizen Technological and Economic Risk Management Natural Risk Sector I-21020 Ispra (VA) Italy.
- Costache, R., Fontanine, F., Corodescu, E., 2014.** Assessment of surface runoff depth changes in S`ar`ațel River basin, Romania using GIS techniques. *Cent. Eur. J. Geosci.*, 6, 363–372.
- Demek, J., 1972.** Manual of detailed geomorphological mapping. Prague: Czechoslovak Academy of Sciences.
- Faniran, A. (1968)** The Index of Drainage Intensity - A Provisional New Drainage Factor, *Australian J of Sci* 31, pp 328-330
- GSMAP, Jaxa Global Rainfall Watch, 2023.** <https://sharaku.eorc.jaxa.jp/GSMaP/index.htm>
- Hassan, A.S., Masoud S.M., 2015.** Geology and geochemistry of Tertiary basalt in south Wadi Hodein area, South Eastern Desert, Egypt. *Arabian J Geo.* doi:10.1007/s12517-012- 0525-6.
- Hong, Y., and Abdelkareem, M., 2022.** Integration of remote sensing and a GIS-based method for revealing prone areas to flood hazards and predicting optimum areas of groundwater resources. *Arab. J. Geosci.*, 15, 1-14.
- Horton, R.E. (1945)** Erosional development of streams and their drainage basins; hydrophysical approach to quantitative morphology. *Bull Geol Soc Am.*, 56, pp. 275–370.
- Ikirri, M., Faik, F., Echogdali, F. Z., Antunes, I. M. H. R., Abioui, M., Abdelrahman, K., Fnais, M. S., Wanaim, A., Id-Belqas, M., Boutaleb, S., Sajinkumar, K. S., and QuesadaRoma´n, A., 2022.** Flood hazard index application in arid catchments: Case of the Taguenit Wadi watershed, Lakhssas, Morocco. *Land*, 11(8), 1178.
- Kirpich, A., 1940.** Time of concentration of small agricultural watershed ASCE. *Civil Eng.* 10(6):1–362
- Lindsay, J.B., Seibert, J. (2013)** Measuring the significance of a divide to local drainage patterns. *Int J Geogr Inf Sci* 27(7):1453–1468.
- Nsangou, D., Kpoumié, A., Mfonka, Z., Ngouh, A.N., Fossi, D.H., Jourdan C., Mbele, H.Z., Mouncherou, O.F., Vandervaere, J., Ngoupayou, J.R., 2022.** Urban flood susceptibility modelling using AHP and GIS approach: case of the Mfoundi watershed at Yaoundé in the South-Cameroon plateau. *Scientific African*, 15, e01043,16pp.
- NWS, 2023.** Flash Flooding Definition. National Weather Service, Philadelphia/Mt Holly, 732Woodlane Rd. Mount Holly, NJ 08060, 609-261-6600 <https://www.weather.gov/phi/FlashFloodingDefinition>
- Nyarko, B.K., 2002.** Application of a rational model in GIS for flood risk assessment in Accra. *J. Spatial Hydrol.*, 2, 1-14.
- Rajkhowa, S. and Sarma, J., 2021.** Climate change and flood risk, global climate change. In Singh, S., Singh, P., S. Rangabhashiyam, P., and Srivastava, K.K., *Global Climate Change Elsevier*. Amsterdam, Netherlands.
- Saaty, T.L., 2008.** Decision making with the analytic hierarchy process. *International Journal of Services Sciences*, 83.

- Sharma, T.P.P., Zhang, J., Khanal, N.R., Prodhan, F.A., Nanzad, L., Zhang, D., and Nepal, P., 2021.** A Geomorphic Approach for Identifying Flash Flood Potential Areas in the East Rapti River Basin of Nepal. *ISPRS Int. J. Geo-Inf.*, 10, 247.
- Soil Conservation Service “SCS”, 1972.** Estimation of direct runoff from storm rainfall, National engineering handbook. Section 4-hydrology, Washington DC, USA; p. 10.1–10.24.
- Souissi, D., Zouhri, L., Hammami, S., Msaddek, M.H., Zghibi, A., Dlala, M., 2019.** GIS-based MCDM—AHP modeling for flood susceptibility mapping of arid areas, southeastern Tunisia. *Geocarto Int.*, 1-25.
- Tehrany, M.S., Pradhan, B., and Jebur, M.N., 2014.** Flood susceptibility mapping using a novel ensemble weights-of-evidence and support vector machine models in GIS. *Journal of hydrology*, 512, 332-343.
- Ullah, K., and Zhang, J., 2020.** GIS-based flood hazard mapping using relative frequency ratio method: A case study of Panjkora River Basin, eastern Hindu Kush, Pakistan. *PLoS ONE*, 15, e0229153.
- Waqas, H., Lu, L., Tariq, A., Li, Q., Baqa, M.F., Xing, J., Sajjad, A., 2021.** Flash Flood Susceptibility Assessment and Zonation Using an Integrating Analytic Hierarchy Process and Frequency Ratio Model for the Chitral District, Khyber Pakhtunkhwa, Pakistan. *Water*, 13, 1650.
- Zaghloul, E., 1996.** Water Resources of Halaib-Shalatien, Final Repoc, NARSS, Cairo, Egypt.